NE 400/500 ABM Project Report

Grayson Gall
Instructor: Dr. Mihai A. Diaconeasa

Due: May 6, 2022

1 Abstract

In designing nuclear reactor systems the specifications of the fuel elements is one of the most important considerations. In this study a spherical fuel elements is considered. The design of which depends on a large number of parameters. In this study several parameters are varied over a range of values to develop the minimum melting temperature of each material under different circumstances. This parametric study also shows which parameters are most important. This is also an important part of the engineering design process as it allows a team of engineers to better understand on which parameters time, effort and money should be spent. Finally, based on this study an "optimum" design is chosen.

Contents

2 Introduction

For this project I have selected a heat conduction analysis of a spherical fuel pellet Option A.4. Numeric values are be based on previous works discussing the design and operation of pebble bed gas cooled reactors. The fuel pellet has a hollow, gas filled center, a section of fuel, another gas filled ring and finally the fuel cladding.

2.1 Geometry

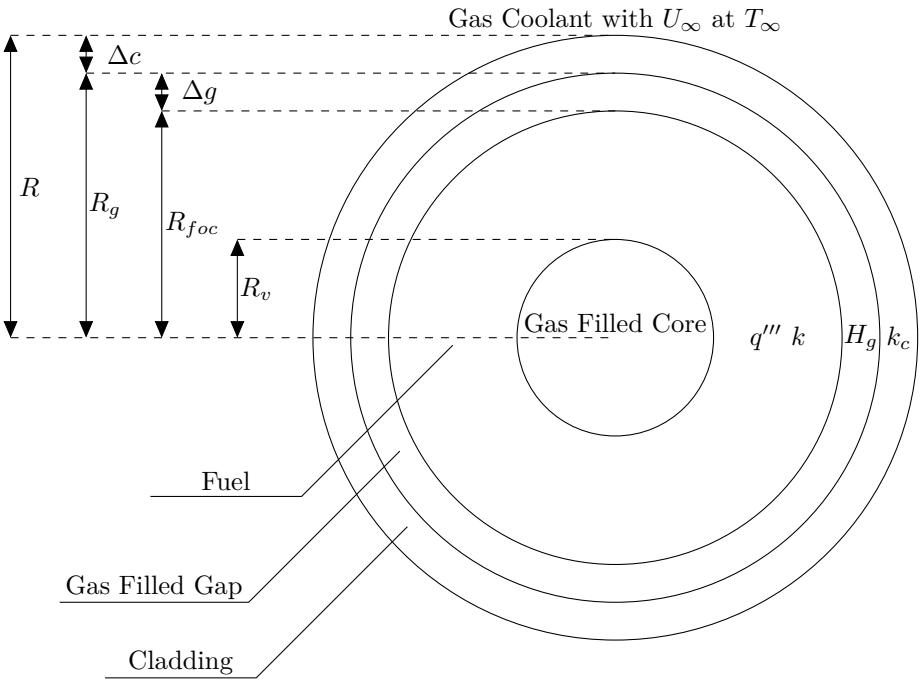

Figure 1: Fuel Pellet Geometry

2.2 Variable Definitions

$$q''' = \text{Volumetric heat generation rate} \tag{1}$$

$$k = \text{Thermal conductivity of the fuel} \tag{2}$$

$$H_G = \text{Thermal resistivity of the Gap} \tag{3}$$

$$k_c = \text{Thermal conductivity of the cladding} \tag{4}$$

$$R_v = \text{Inner fuel radius} \tag{5}$$

$$R_{foc} = \text{Outer fuel radius} \tag{6}$$

$$R_G = \text{Inner cladding radius} \tag{7}$$

$$R = \text{Outer cladding radius} \tag{8}$$

$$\Delta g = \text{Gap Width} \tag{9}$$

$$\Delta c = \text{Cladding Thickness} \tag{10}$$

$$U_\infty = \text{Gas Coolant Velocity} \tag{11}$$

$$T_\infty = \text{Gas Coolant Bulk Temperature} \tag{12}$$

3 Theory

It is assumed that the system is at steady state. It is also assumed that the volumetric heat generation rate is uniform making the temperature profile purely a function of radial position.

3.1 Fuel Region

$$\frac{1}{r^2}\frac{\partial}{\partial r}\left(r^2 k\frac{\partial T}{\partial r}\right) = -q''' \tag{13}$$

It is also assumed that the temperature profile is symmetric which can be captured in a boundary condition at the inner fuel radius.

$$\left.\frac{\partial T}{\partial r}\right|_{r=R_v} = 0 \tag{14}$$

$$\int \frac{\partial}{\partial r}\left(r^2 k\frac{\partial T}{\partial r}\right) dr = -\int q''' r^2 dr \tag{15}$$

$$r^2 k\frac{\partial T}{\partial r} = -\frac{q'''}{3}r^3 + C_1 \tag{16}$$

$$\frac{\partial T}{\partial r} = -\frac{q'''}{3k}r + \frac{C_1}{k}\frac{1}{r^2} \tag{17}$$

Applying the boundary condition at the inner radius a value for C_1 can be obtained.

$$0 = -\frac{q'''}{3k}R_v + \frac{C_1}{k}\frac{1}{R_v^2} \tag{18}$$

$$C_1 = \frac{q'''}{3k}R_v^3 \tag{19}$$

$$\frac{\partial T}{\partial r} = -\frac{q'''}{3k}r + \frac{q'''}{3k}\frac{R_v^3}{r^2} \tag{20}$$

$$\int \frac{\partial T}{\partial r} dr = \int -\frac{q'''}{3k}r + \frac{q'''}{3k}\frac{R_v^3}{r^2} dr \tag{21}$$

$$T(r) = -\frac{q'''}{6k}r^2 - \frac{q'''}{3k}\frac{R_v^3}{r} + C_2 \tag{22}$$

$$T(r) = C_2 - \frac{q'''}{6k}\left(r^2 + 2\frac{R_v^3}{r}\right) \tag{23}$$

3.2 Gap Region

The heat flux across the gap can be expressed in terms of the temperature difference and the gap conductance.

$$q''\left(R_G\right) = H_g\left(T\left(R_{foc}\right) - T\left(R_G\right)\right) \tag{24}$$

This gives a relation for the temperature drop across the gap.

$$T\left(R_{foc}\right) - T\left(R_G\right) = \frac{q''\left(R_G\right)}{H_G} \tag{25}$$

The heat flux at the inner clad surface can then be related to the heat flux at the outer clad surface.

$$q''\left(R_G\right) = q''\left(R_{foc}\right)\frac{R_{foc}}{R_G} \tag{26}$$

The temperature drop across the gap can be written in the form of equation 27

$$T\left(R_{foc}\right) - T\left(R_G\right) = \frac{q''\left(R_{foc}\right)R_{foc}}{H_G\ R_G} \tag{27}$$

Using Fourier's law of heat conduction and the temperature profile developed in the fuel region the heat flux at the edge of the fuel can be written in term of the volumetric heat generation rate.

$$q''\left(R_{foc}\right) = -k\frac{\partial T}{\partial r}\bigg|_{r=R_{foc}} \tag{28}$$

$$q''\left(R_{foc}\right) = -k\left(-\frac{q'''}{3k}R_{foc} + \frac{q'''}{3k}\frac{R_v^3}{R_{foc}^2}\right) \tag{29}$$

The temperature drop across the gap can then be re-written using equation 29.

$$T\left(R_{foc}\right) - T\left(R_G\right) = -k\left(-\frac{q'''}{3k}R_{foc} + \frac{q'''}{3k}\frac{R_v^3}{R_{foc}^2}\right)\frac{R_{foc}}{H_G\ R_G} \tag{30}$$

$$T\left(R_{foc}\right) - T\left(R_G\right) = -\frac{q'''}{3H_G\ R_G}\left(\frac{R_v^3}{R_{foc}} - R_{foc}^2\right) \tag{31}$$

$$T\left(R_{foc}\right) = T\left(R_G\right) - \frac{q'''}{3H_G\ R_G}\left(\frac{R_v^3}{R_{foc}} - R_{foc}^2\right) \tag{32}$$

Using equation 32 an expression for the second constant C_2 can then be developed.

$$T(R_{foc}) = C_2 - \frac{q'''}{6}\left(R_{foc}^2 + 2\frac{R_v^3}{R_{foc}}\right) \tag{33}$$

$$T\left(R_G\right)-\frac{q'''}{3H_G\ R_G}\left(\frac{R_v^3}{R_{foc}}-R_{foc}^2\right)=C_2-\frac{q'''}{6}\left(R_{foc}^2+2\frac{R_v^3}{R_{foc}}\right) \tag{34}$$

$$C_2=T\left(R_G\right)-\frac{q'''}{3H_G\ R_G}\left(\frac{R_v^3}{R_{foc}}-R_{foc}^2\right)+\frac{q'''}{6}\left(R_{foc}^2+2\frac{R_v^3}{R_{foc}}\right) \tag{35}$$

3.3 Cladding Region

$$\frac{1}{r^2}\frac{\partial}{\partial r}\left(r^2 k_c \frac{\partial T}{\partial r}\right) = 0 \tag{36}$$

$$\frac{\partial}{\partial r}\left(r^2 k_c \frac{\partial T}{\partial r}\right) = 0 \tag{37}$$

$$\int \frac{\partial}{\partial r}\left(r^2 k_c \frac{\partial T}{\partial r}\right) dr = \int 0 dr \tag{38}$$

$$r^2 k_c \frac{\partial T}{\partial r} = C_3 \tag{39}$$

$$\frac{\partial T}{\partial r} = \frac{C_3}{k_c r^2} \tag{40}$$

$$\int \frac{\partial T}{\partial r} dr = \int \frac{C_3}{k_c r^2} dr \tag{41}$$

$$T(r) = -\frac{C_3}{k_c r} + C_4 \tag{42}$$

Using newtons law of cooling and the relation established between the heat flux at the cladding inner wall and fuel outer wall the heat flux at at the inner cladding wall can written as equation 43.

$$q''(R_G) = -k_c \left.\frac{\partial T}{\partial r}\right|_{r=R_G} \tag{43}$$

$$q''(R_G) = q''(R_{foc})\frac{R_{foc}}{R_G} \tag{44}$$

$$q''(R_{foc}) = -k\left(-\frac{q'''}{3k}R_{foc} + \frac{q'''}{3k}\frac{R_v^3}{R_{foc}^2}\right) \tag{45}$$

$$q''(R_G) = -k\left(-\frac{q'''}{3k}R_{foc} + \frac{q'''}{3k}\frac{R_v^3}{R_{foc}^2}\right)\frac{R_{foc}}{R_G} \tag{46}$$

$$-k_c \left.\frac{\partial T}{\partial r}\right|_{r=R_G} = -k\left(-\frac{q'''}{3k}R_{foc} + \frac{q'''}{3k}\frac{R_v^3}{R_{foc}^2}\right)\frac{R_{foc}}{R_G} \tag{47}$$

$$\left.\frac{\partial T}{\partial r}\right|_{r=R_G} = \frac{k}{k_c}\left(-\frac{q'''}{3k}R_{foc} + \frac{q'''}{3k}\frac{R_v^3}{R_{foc}^2}\right)\frac{R_{foc}}{R_G} \tag{48}$$

With this condition C_3 is then obtained.

$$\left.\frac{\partial T}{\partial r}\right|_{r=R_G} = \frac{C_3}{k_c R_G^2} = \frac{k}{k_c}\left(-\frac{q'''}{3k}R_{foc} + \frac{q'''}{3k}\frac{R_v^3}{R_{foc}^2}\right)\frac{R_{foc}}{R_G} \tag{49}$$

$$C_3 = R_G^2 k \left(-\frac{q'''}{3k} R_{foc} + \frac{q'''}{3k} \frac{R_v^3}{R_{foc}^2} \right) \frac{R_{foc}}{R_G} \tag{50}$$

$$C_3 = \frac{q''' R_G}{3} \left(\frac{R_v^3}{R_{foc}} - R_{foc}^2 \right) \tag{51}$$

$$\frac{\partial T}{\partial r} = \frac{q''' R_G}{3k_c} \left(\frac{R_v^3}{R_{foc}} - R_{foc}^2 \right) \frac{1}{r^2} \tag{52}$$

Using Newtons Law of cooling to establish the a boundary condition at the outer cladding radius the system of equations can be closed.

$$-k_c \left. \frac{\partial T}{\partial r} \right|_{r=R} = h_c \left(T(R) - T_\infty \right) \tag{53}$$

$$-k_c \frac{q''' R_G}{3k_c} \left(\frac{R_v^3}{R_{foc}} - R_{foc}^2 \right) \frac{1}{R^2} = h_c \left(T(R) - T_\infty \right) \tag{54}$$

$$T(R) = T_\infty - \frac{q''' R_G}{3h_c} \left(\frac{R_v^3}{R_{foc}} - R_{foc}^2 \right) \frac{1}{R^2} \tag{55}$$

The final unknown coefficient can then be obtained.

$$T(r) = -\frac{q''' R_G}{3k_c} \left(\frac{R_v^3}{R_{foc}} - R_{foc}^2 \right) \frac{1}{r} + C_4 \tag{56}$$

$$-\frac{q''' R_G}{3k_c} \left(\frac{R_v^3}{R_{foc}} - R_{foc}^2 \right) \frac{1}{R} + C_4 = T_\infty - \frac{q''' R_G}{3h_c} \left(\frac{R_v^3}{R_{foc}} - R_{foc}^2 \right) \frac{1}{R^2} \tag{57}$$

$$C_4 = T_\infty - \frac{q''' R_G}{3h_c} \left(\frac{R_v^3}{R_{foc}} - R_{foc}^2 \right) \frac{1}{R^2} + \frac{q''' R_G}{3k_c} \left(\frac{R_v^3}{R_{foc}} - R_{foc}^2 \right) \frac{1}{R} \tag{58}$$

$$C_4 = T_\infty + \frac{q''' R_G}{3} \left(\frac{R_v^3}{R_{foc}} - R_{foc}^2 \right) \left(\frac{1}{k_c R} - \frac{1}{h_c R^2} \right) \tag{59}$$

With these fully developed temperature profiles in each region the melting temperatures for the fuel and the cladding can be obtained. These melting temperatures will simply be the maximum temperatures in each respective region.

3.4 Heat transfer coefficient

The heat convective heat transfer coefficient can be obtained from the Nusselt number.

$$Nu = \frac{h_c 2R}{k_{\text{fluid}}} \tag{60}$$

And for flow around a sphere the relation for Nusselt is obtained from [4].

$$Nu = CRe^m Pr^{1/3} \tag{61}$$

Re	C	m
4e-1-4	0.989	0.33
4-4e1	0.911	0.385
4e1-4e3	0.683	0.466
4e3-4e4	0.193	0.618
4e4-4e5	0.027	0.805

Table 1: Nusselt number parameters for various Re

$$h_c = \frac{k_{\text{fluid}}}{2R} CRe^m Pr^{1/3} \tag{62}$$

$$Pr = \frac{C_p \mu}{k_{\text{fluid}}} \tag{63}$$

$$Re = \frac{G2R}{\mu} \tag{64}$$

4 Methods

In order to conduct a parametric study of the temperature profile in various fuel pellet designs MATLAB was used to implement the equations developed in section 3. MATLAB was selected as the language of choice because of my familiarity with the language and the convenient features. While MATLAB is not the fastest or most efficient language this problem does not require large computations so performance was an important consideration.

4.1 Pseudocode

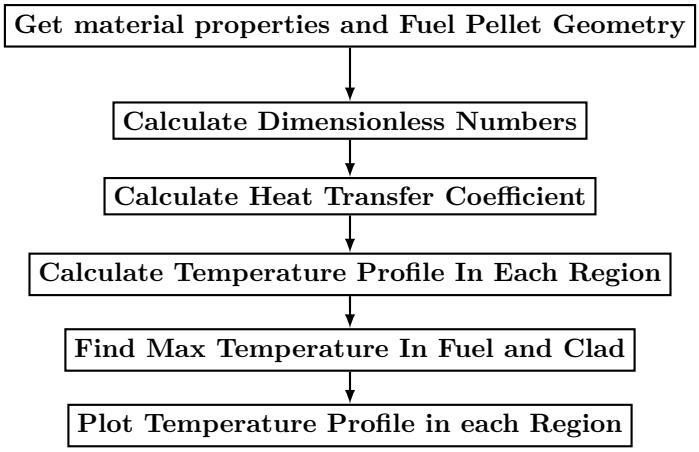

4.2 Code Usage

All of the functions and the proper directory setup can be unpacked by unzipping the zip file attached with the submission of this report. Ensure that the version of MATLAB you are using is compatible with live scripts. To run the code open the file "main.mlx" and run using the run button on the "Live Editor/Run" section or run which ever section is of interest. Running this code will not only generate output to the live script but it will also create a text file "tex.txt" This file contains auto generated latex code for the results section. In addition to this running the code will also create a folder called "figFolder" this folder will contain a pdf version of every figure used in the results section.

5 Numeric Parameters

In order to fully characterize this parametric study the ranges for each quantity that will be varied must first be determined. The values used in the parametric studies for each parameter are discussed in this section. First, the materials for this fuel pebble must be determined. Based on [10] and [13]: The gas coolant is treated as Helium, the fuel region is treated as Uranium Oxycarbide with material properties based on the work in [2], and the cladding is treated as Pyrolytic Carbon with material properties based on the work in [15]. The gas filled gap is also be treated a helium, however, the gap resistivity is based on material presented in [3] while this value is presented for Light Water Reactor Systems I was unable to find this value in literature. The gap resistivity presented in the course thus serves as the best estimate for this quantity.

5.1 Gas Coolant

5.1.1 Coolant Temperature

The coolant temperatures are based on the values presented in [13] and [8] for helium cooled pebble bed reactors core inlet temperatures temperatures are between 250°C and 400°C. While core outlet temperatures are between $750°C$ and 1000°C. In order to obtain a base case temperature within this region I take the core inlet temperature to be 325°C and the core outlet temperature of 875°C both are the average of the upper and lower bounds of the temperature regimes. I then assume that bulk coolant temperature in the core at the location of the pebble of interest is the average between these two values at 600°C. This serves as my base test case and I vary the coolant temperature ±100°C in increments of 50 °C for a total of 5 different coolant temperatures.

$$T_\infty = \begin{cases} 500 \\ 550 \\ 600 \\ 650 \\ 700 \end{cases} \quad [°\mathrm{C}] \tag{65}$$

When varying other parameters in this study I hold the coolant temperature constant at 600°C.

5.1.2 Coolant Properties

The value presented in [8] gives a reactor core diameter of 5.6 m. This value is held constant and the coolant velocity is varied. The dynamic viscosity is also held constant at 600°C in all calculations. This is done because the helium dynamic viscosity's do not vary significantly with in the temperature range of interest. The same is true for the thermal conductivity of helium. Values presented for the dynamic viscosity were obtained from [7] and values for thermal conductivity are obtained from [12].

$$\mu = 4.18e-5 \left[\frac{\text{kg}}{\text{m}^2\ \text{s}}\right] \tag{66}$$

$$k_{\text{fluid}} = 0.3218 \left[\frac{\text{W}}{\text{m K}}\right] \tag{67}$$

The value for the specific heat of helium was found from [1].

$$C_p = 5.193e3 \left[\frac{\text{J}}{\text{kg K}}\right] \tag{68}$$

The density also does not vary significantly within the temperature range of interest and as such is treated as a constant at 600°C obtained from [12].

$$\rho = 0.05763 \left[\frac{\text{kg}}{\text{m}^3}\right] \tag{69}$$

$$U_\infty = \frac{G}{\rho} \left[\frac{\text{m}}{s}\right] \tag{70}$$

5.1.3 Coolant Velocity

The reactor fluid velocity is varied such that each region of flow presented in table 1 is utilized.

$$U_\infty = \begin{cases} 1.2089e-2 \\ 1.2089e-1 \\ 1.2089e \\ 1.2089e2 \\ 1.2089e3 \end{cases} \quad \left[\frac{\text{m}}{\text{s}}\right] \tag{71}$$

5.2 Fuel Pellet Cladding

Based on the values presented in [15] a constant cladding thermal conductivity is used.

$$k_c = 8.11 \left[\frac{\text{W}}{\text{m K}}\right] \tag{72}$$

In [10] the cladding thickness on fuel pellets is given to be 5mm. This will be the base value used in the parametric study.

$$\Delta c = \begin{cases} 3 \\ 4 \\ 5 \\ 6 \\ 7 \end{cases} \quad [10^{-3}\text{m}] \tag{73}$$

The gap thickness and fuel region outer radius will be held constant at their respective base cases.

5.3 Gas Filled Gap

Consistent with the material presented in [3] the gap thermal Resistance is varied within 2 orders of magnitude.

$$H_g = \begin{cases} 5.6e1 \\ 5.6e2 \\ 5.6e3 \\ 5.6e4 \\ 5.6e5 \end{cases} \quad \left[\frac{\mathrm{W}}{\mathrm{m}^2\ \mathrm{K}}\right] \tag{74}$$

With the assumption that the clad thickness and the gap thickness are similar. Those parameters will be varied across the same values.

$$\Delta g = \begin{cases} 3 \\ 4 \\ 5 \\ 6 \\ 7 \end{cases} \quad \left[10^{-3}\mathrm{m}\right] \tag{75}$$

The fuel region and cladding thickness will be help constant at their respective base case values.

5.4 Fuel Region

The thermal conductivity of the fuel is also held constant at at the value given in [2]. The value being used is valid temperatures between 1187-2007°C. I have selected this value because this range should cover the fuel temperatures being studied and outside this region its value does not vary significantly

$$k = 17 \left[\frac{\mathrm{W}}{\mathrm{m\ K}}\right] \tag{76}$$

Consistent with [10] the base value for the fuel outer radius is 50 mm. This does not have the inner gas filled core and I will set that value at a constant value of 5 mm.

$$R_{foc} = \begin{cases} 30 \\ 40 \\ 50 \\ 60 \\ 70 \end{cases} \quad \left[10^{-3}\mathrm{m}\right] \tag{77}$$

$$R_v = 10e - 3\,[\mathrm{m}] \tag{78}$$

The gap and cladding thickness will be help constant at their respective base values.

5.5 Volumetric Heat Generation Rate

In order to calculate the volumetric heat generation rate it will be assumed that each spherical fuel pellet contributes equally to the total thermal power of the reactor. Values presented in [8] give the total reactor thermal power of 750 [MW] and 675,000 fuel pellets. This serves as the base case of the volumetric heat generation rate for each pellet.

$$q''' = \frac{\dot{Q}}{n\frac{4}{3}\pi R^3} \tag{79}$$

Where n is the number of fuel pellets.

$$q''' = \begin{cases} 1.028 \\ 1.128 \\ 1.228 \\ 1.328 \\ 1.428 \end{cases} \quad \left[10^6 \frac{\mathrm{W}}{\mathrm{m}^3}\right] \tag{80}$$

6 Results

In this section the results of the parametric studies over the parameters that were discussed in section 5 are presented. Each study contains a plot of the temperature distribution from the inner fuel radius to the outer cladding radius. For these studies there is one parameters that was varied while all others were held constant at their respective base case values. For the gap region a linear shape is assumed. Below the graphs is a table that presents the maximum temperature reached in each fuel region. These temperatures correspond to the minimum required melting temperature of the material in each region. These temperatures are presented in the same order that appear in the legend on each plot.

6.1 Base Case

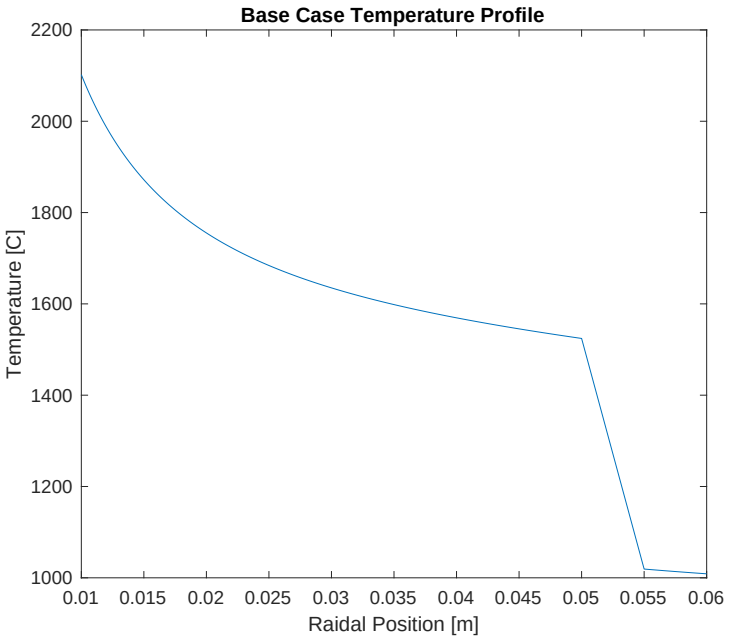

Figure 2: Base Case Temperature Profile

Fuel Melt Temperature [$^{\circ}C$]	Clad Melt Temperature [$^{\circ}C$]
2102.0386	1019.1844

Table 2: Minimum Melting Temperatures for each region

6.2 Coolant Temperature Parametric Study

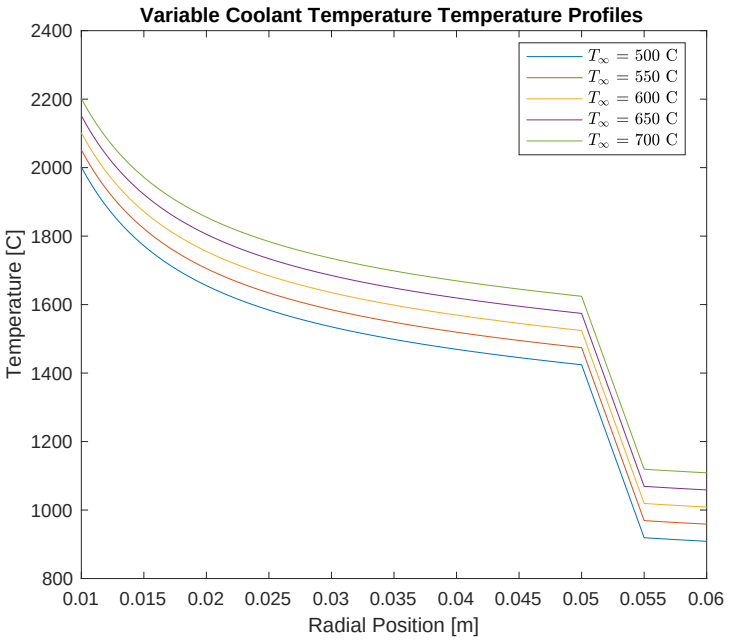

Figure 3: Parametric Study of Coolant Temperature

Fuel Melt Temperature [$^\circ C$]	Clad Melt Temperature [$^\circ C$]
2002.0386	919.1844
2052.0386	969.1844
2102.0386	1019.1844
2152.0386	1069.1844
2202.0386	1119.1844

Table 3: Minimum Melting Temperatures for each region

6.3 Coolant Velocity Parametric Study

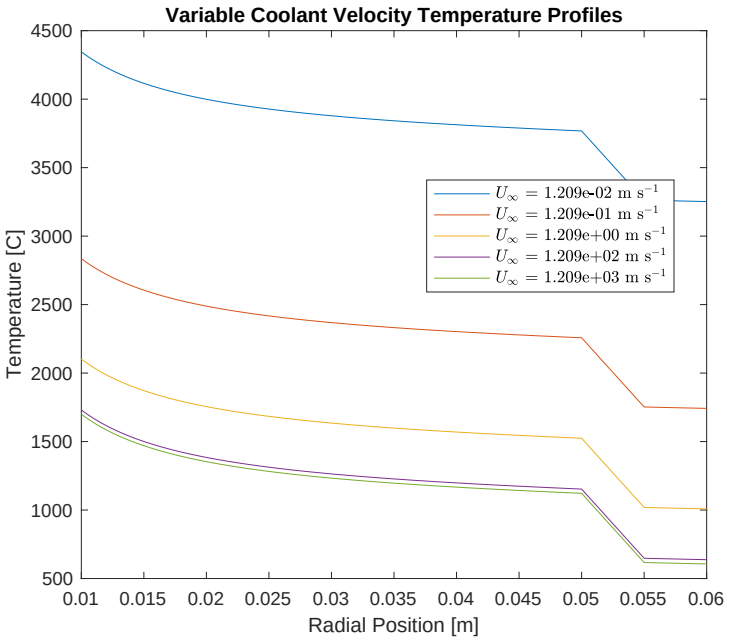

Figure 4: Parametric Study of Coolant Velocity

Fuel Melt Temperature [$^\circ C$]	Clad Melt Temperature [$^\circ C$]
4345.6141	3262.7599
2835.5005	1752.6463
2102.0386	1019.1844
1730.8319	647.9776
1699.8845	617.0302

Table 4: Minimum Melting Temperatures for each region

6.4 Cladding Thickness Parametric Study

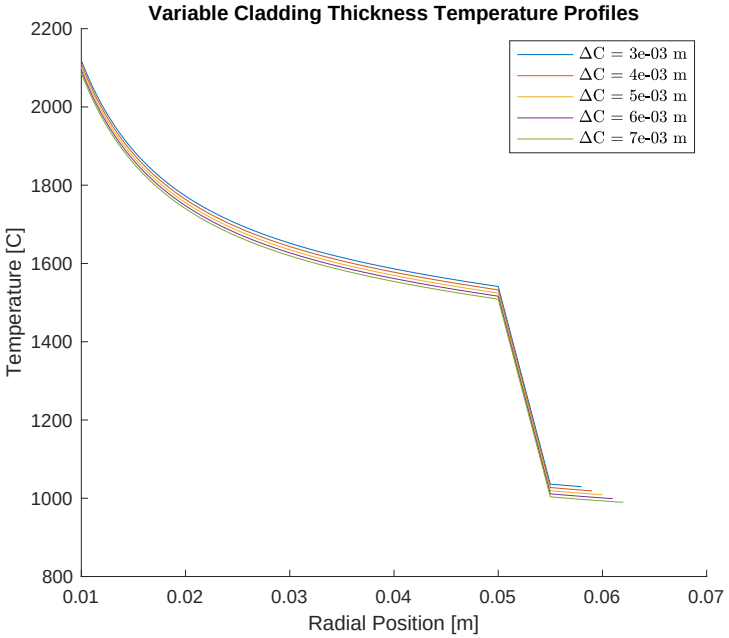

Figure 5: Parametric Study of Cladding Thickness

Fuel Melt Temperature [$^{\circ}C$]	Clad Melt Temperature [$^{\circ}C$]
2118.9101	1036.0558
2110.2903	1027.4360
2102.0386	1019.1844
2094.1339	1011.2796
2086.5562	1003.7019

Table 5: Minimum Melting Temperatures for each region

6.5 Gap Conductance Parametric Study

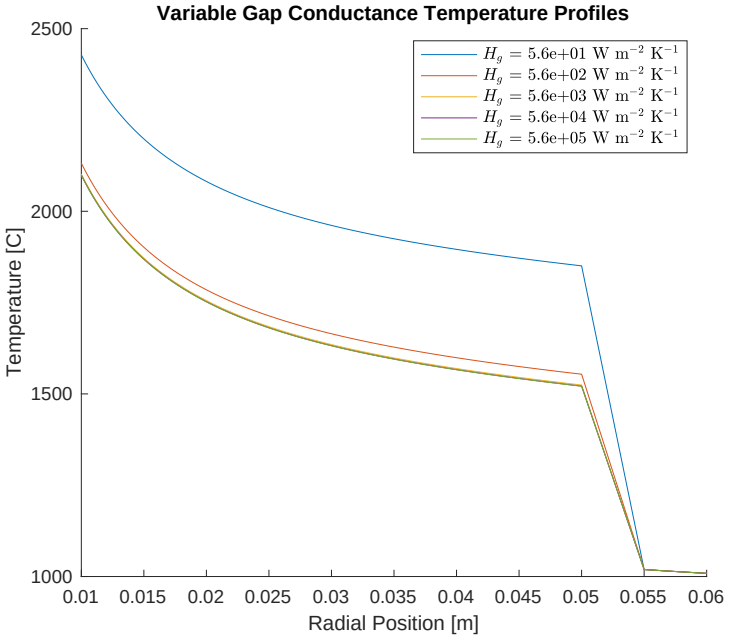

Figure 6: Parametric Study of Gap Resistance

Fuel Melt Temperature [$^{\circ}C$]	Clad Melt Temperature [$^{\circ}C$]
2428.3484	1019.1844
2131.7032	1019.1844
2102.0386	1019.1844
2099.0722	1019.1844
2098.7755	1019.1844

Table 6: Minimum Melting Temperatures for each region

6.6 Gap Thickness Parametric Study

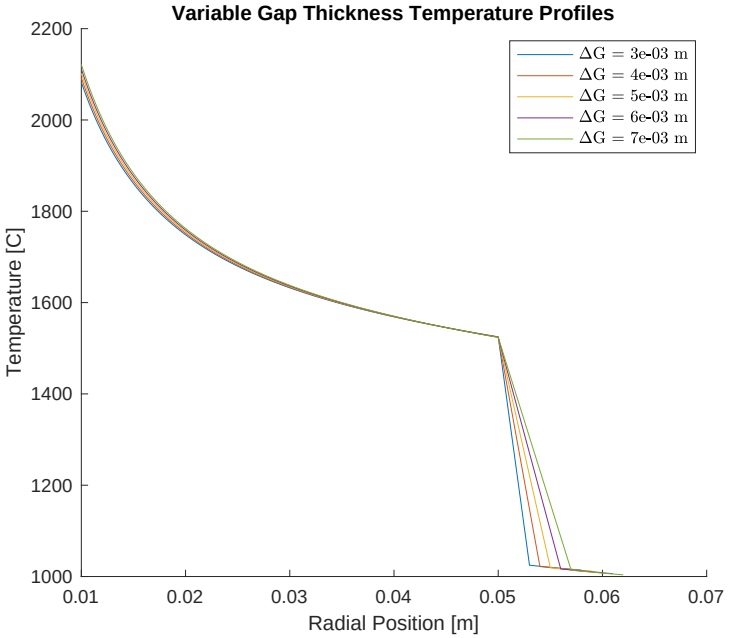

Figure 7: Parametric Study of Gap Thickness

Fuel Melt Temperature [$^{\circ}C$]	Clad Melt Temperature [$^{\circ}C$]
2082.6944	1024.7511
2092.3380	1021.9404
2102.0386	1019.1844
2111.7946	1016.4815
2121.6041	1013.8301

Table 7: Minimum Melting Temperatures for each region

6.7 Fuel Outer Radius Parametric Study

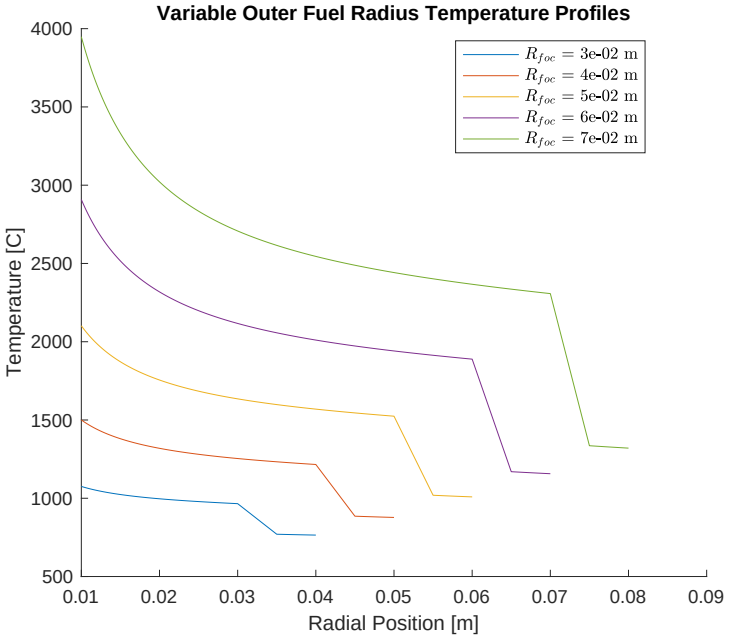

Figure 8: Parametric Study of Outer Fuel Radius

Fuel Melt Temperature [$^{\circ}C$]	Clad Melt Temperature [$^{\circ}C$]
1075.5886	770.1768
1500.3227	885.4219
2102.0386	1019.1844
2908.5634	1169.7241
3948.4829	1335.6502

Table 8: Minimum Melting Temperatures for each region

6.8 Volumetric Heat Generation Rate Parametric Study

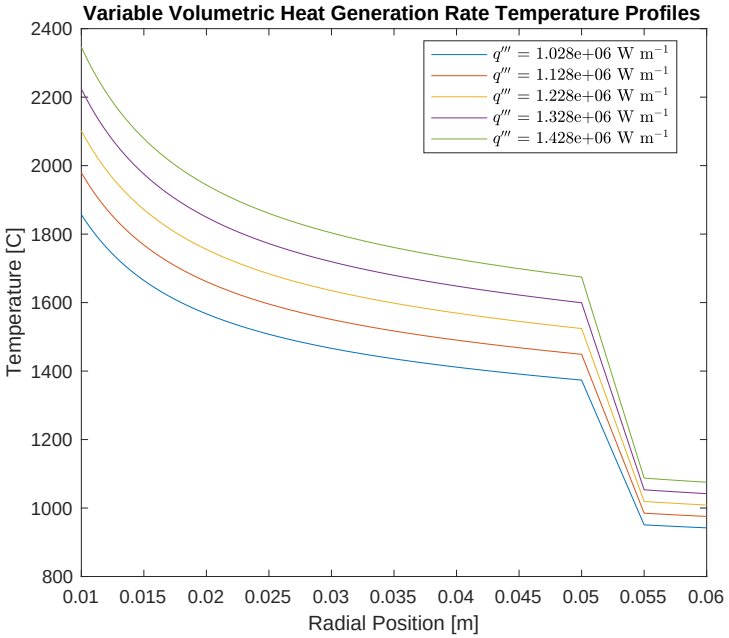

Figure 9: Parametric Study of Volumetric Heat Generation Rate

Fuel Melt Temperature [$^{\circ}C$]	Clad Melt Temperature [$^{\circ}C$]
1857.3584	950.8998
1979.6695	985.0340
2101.9807	1019.1682
2224.2918	1053.3024
2346.6029	1087.4366

Table 9: Minimum Melting Temperatures for each region

7 Discussion

7.1 Base Case

Based on the work [14] the melting temperature of the Uranium Oxycarbide is 2500°C. Based on [11] the melting temperature of the Pyrolytic Carbon is at least above 1700°C - 1800°C. Starting with the base case for all parameters the maximum temperature in the fuel is well below the melting temperature of the fuel. Additionally, the maximum temperature in the cladding region is also far below the melting temperature of the cladding.

7.2 Coolant Temperature Parametric Study

In varying the coolant temperature it is seen that the maximum temperature reached in the fuel region is approximately 300°C from the melting temperature of the fuel. While there is still a buffer between the maximum allowable temperature and the maximum achieved temperature this buffer may not meet safety specifications since it is relatively close. However, there is still nearly 600°C between the maximum clad temperature and the clad melting temperature so this temperature would be well within safe operational specifications. From this study and the equations developed in section 3 it is observed that the maximum temperature increases directly with the coolant temperature. However, the variation observed due to the coolant temperature keeps the maximum temperatures well within the melting temperatures so this dependence is not vary significant in the temperature ranges being studied.

7.3 Coolant Velocity Parametric Study

Because the coolant velocity appears in the expressions for the convective heat transfer coefficient the relationship between the coolant velocity and the temperatures achieved in the fuel pellet is highly nonlinear. Very low fluid velocities lead to temperatures that would melt the fuel pellet and the cladding very quickly. The effect that the fluid velocity can have on the temperatures achieved in the fuel pellet seems to approach a lower bound on maximum fuel temperature asymptotically. This shows that there is a point after which increasing the fluid velocity will be harder than meaningfully impactful to temperature profiles. This means that when designing a full reactor system there exists a practically achievable and impactful upper bound on fluid velocity.

7.4 Cladding Thickness Parametric Study

From the results it is clear that the cladding thickness does not have any significant effects on the temperature profiles. It does vary the temperatures within more than 30°C between the lowest and highest temperatures in each region. While it was not studied in this work one parameter that would be of interest for future works is a variation of the thermal conductivity of the cladding. It might

be expected that varying the thermal conductivity would have a much larger impact on the overall temperature profile then varying the cladding thickness.

7.5 Gap Conductance Parametric Study

As would be expected the gap conductance has a large impact on the temperature profile in the fuel region and varies the maximum fuel temperature achieved. Although increasing the cap conductance can only have such a large impact on the maximum fuel temperature. The lower bound on the maximum fuel temperature seems to be approached asymptotically with increasing gap conductance. This means that increasing the gap conductance will only be useful to a certain extent.

7.6 Gap Thickness Parametric Study

Similarly to the cladding thickness increasing the gap thickness has very little impact on the temperature profile in the fuel pellet. This was a result that I was surprised to see as I thought that increasing the gap distance would display a similar relationship to that of increasing the gap conductance.

7.7 Fuel Outer Radius Parametric Study

As expected the outer fuel radius seems to have the largest impact on the temperatures achieved in each region. Even increasing the fuel radius by 1 cm puts the maximum fuel temperature beyond the melting temperature of the fuel. This to be expected since the relationship between the total heat generation rate in the fuel is cubically proportional to the outer fuel radius. However, none of the fuel radii put the maximum cladding temperature outside the melting region for the cladding material.

7.8 Volumetric Heat Generation Rate Parametric Study

The variation in the volumetric heat generation rate displays a similar relationship to that of the fluid velocity. However, the variation in the temperatures has a much larger effect on the maximum temperatures than the fluid velocity. This is to be expected but I was surprised that this did not have as large an effect on the temperature profile as the variation in the outer fuel radius. However, I believe this is because the volumetric heat generation rate has a linearly relationship to the total heat generated as opposed to the cubic relationship of the radius.

8 Conclusion

There are many parameters to considers when designing a fuel element for a reactor system. However, not all design elements are created equal. Over the course of this parametric study it was shown that outer fuel radius R_{foc} is the most dominant property of those studied. Following outer fuel radius in dominance are gap conductance H_g and the coolant velocity U_∞. These properties are then followed by the volumetric heat generation rate q''' and the coolant temperature T_∞. The gap thickness Δg and the cladding thickness Δc were seen to effect the temperature distribution the least. There are still other properties that could be varied in future works and those studied in this report are not exhaustive. Some properties that may be of interest in the future are the thermal conductivities of both the fuel and the cladding k and k_c as well as any of the fluid properties or even consideration of other fluids entirely. The fluid velocities used in this study do not necessarily reflect realistic fluid velocities, however, further reading and other correlations would be needed to discuss fluid velocities with larger orders of magnitude. Finally, the best combination of parameters based on those varied would be the case studied with the highest fluid velocity, $U_\infty = 1.209e3$ m / s. This was selected as the best combination while maintaining the same base case power level because it is combination that decreased the maximum clad and the fuel temperatures the most at the given base power level.

9 References

[1] Author. *Helium - specific heat, latent heat of fusion, latent heat of vaporization*. Nov. 2021. URL: https://www.nuclear-power.com/helium-specific-heat-latent-heat-vaporization-fusion/#:~:text=Specific%5C%20heat%5C%20of%5C%20Helium%5C%20is%5C%205.193%5C%20J%5C%2Fg%5C%20K..

[2] J L Bates. "THERMAL CONDUCTIVITY AND ELECTRICAL RESISTIVITY OF URANIUM OXYCARBIDE." In: (Jan. 1969). DOI: 10.2172/4776323. URL: https://www.osti.gov/biblio/4776323.

[3] Dr. Mihai A. Diaconeasa. *Lecture 2.4 Heat Conduction in Reactor Elements - Light Water Reactor Fuel Elements*. NC State University, Department of Nuclear Engineering. 2022.

[4] Dr. Mihai A. Diaconeasa. *Lecture 3.2 Heat Conduction in Reactor Elements - Light Water Reactor Fuel Elements*. NC State University, Department of Nuclear Engineering. 2022.

[5] Dr. Mihai A. Diaconeasa. *Ne 400/500 Lecture Notes*. NC State University, Department of Nuclear Engineering. 2022.

[6] Dr. Mihai A. Diaconeasa. *NE 500 Project Guidelines*. NC State University, Department of Nuclear Engineering. 2022.

[7] *Gases - dynamic viscosities*. URL: https://www.engineeringtoolbox.com/gases-absolute-dynamic-viscosity-d_1888.html.

[8] R.A. Moore, M.E. Kantor, H.L. Brey, and H.G. Olson. "HTGR experience, programs, and future applications". In: *Nuclear Engineering and Design* 72.2 (1982), pp. 153–174. ISSN: 0029-5493. DOI: https://doi.org/10.1016/0029-5493(82)90212-6. URL: https://www.sciencedirect.com/science/article/pii/0029549382902126.

[9] Mujid S. Kazimi Neil E. Todreas. *Nuclear Systems Volume 1 Thermal Hydraulic Fundamentals*. 6000 Broken Sound Parkway NW, Suite 300 Boca Raton, FL 33487-2742: Taylor & Francis Group, LLC, 2011.

[10] NRC. *NRC: ML12045A014 - Nuclear Regulatory Commission*. URL: https://www.nrc.gov/docs/ML1204/ML12045A014.pdf.

[11] Christian M. Petrie, Kurt Smith, and Tyler Gerczak. *Design and Thermal Analysis for Irradiation of Pyrolytic Carbon / Silicon Carbide Diffusion Couples in the High Flux Isotope Reactor*. Oak Ridge National Lab. URL: https://info.ornl.gov/sites/publications/Files/Pub1043.pdf.

[12] *Thermophysical properties of helium (he) calculator*. URL: https://www.thermosolver.com/properties_of_He.

[13] Shohei Ueta, Jun Aihara, Kazuhiro Sawa, Atsushi Yasuda, Masaki Honda, and Noboru Furihata. "Development of high temperature gas-cooled reactor (HTGR) fuel in Japan". In: *Progress in Nuclear Energy* 53.7 (2011). The Third International Symposium on Innovative Nuclear Energy Systems, INES-3- Innovative Nuclear Technologies for Low-Carbon Society, pp. 788–793. ISSN: 0149-1970. DOI: https://doi.org/10.1016/j.pnucene.2011.05.005. URL: https://www.sciencedirect.com/science/article/pii/S0149197011000928.

[14] *URANIUM CARBIDE AS A NUCLEAR FUEL*. IAEA. URL: https://inis.iaea.org/collection/NCLCollectionStore/_Public/03/026/3026030.pdf.

[15] Yuzhou Wang, David H. Hurley, Erik P. Luther, Miles F. Beaux, Douglas R. Vodnik, Reuben J. Peterson, Bryan L. Bennett, Igor O. Usov, Pengyu Yuan, Xinwei Wang, and Marat Khafizov. "Characterization of ultralow thermal conductivity in anisotropic pyrolytic carbon coating for thermal management applications". In: *Carbon* 129 (2018), pp. 476–485. ISSN: 0008-6223. DOI: https://doi.org/10.1016/j.carbon.2017.12.041. URL: https://www.sciencedirect.com/science/article/pii/S0008622317312745.